Research on Chemical Intermediates (2019) 45:2403–2427
https://doi.org/10.1007/s11164-019-03741-3

Photophysical and antimicrobial properties of new double-armed benzo-15-crown-5 ligands and complexes

Serhat Koçoğlu[1,2] · Hatice Ogutcu[3] · Zeliha Hayvalı[1]

Received: 28 September 2018 / Accepted: 12 January 2019 / Published online: 24 January 2019

Abstract

New double-armed crown ether ligands linked to pyridine derivatives have been synthesized and characterized. These macrocyclic ligands (**1**–**5**) have been synthesized by the reactions of 4′,5′-bis(bromomethyl)benzo-15-crown-5 with 3-hydroxy pyridine derivatives. A series of Na^+, K^+ and Ag^+ complexes (**1a**–**5a**, **1b**–**5b** and **1c**–**5c**) of the macrocyclic ligands have been prepared from sodium perchlorate, sodium picrate, potassium iodide, potassium picrate and silver nitrate salts, respectively. The most suitable cation Na^+ is bound to the 15-crown-5 cavity and 1:1 "filling complexes" are formed (**1a**–**5a**) while the K^+ cation interacts with the crown ether cavity and forms sandwich-type complexes (**1b**–**5b**). The Ag^+ complexes (**1c**–**5c**) have been obtained with a pyridine moiety of the new crown ethers. New ligands undergo photophysical changes when bonding the cation. The influence of metal cations such as Na^+, Li^+, K^+, Fe^{3+}, Cu^{2+}, Ca^{2+}, Ba^{2+} and Al^{3+} on the spectroscopic properties of the pyridine linked to the double-armed crown ether moiety was investigated in EtOH solution by means of absorption and emission spectrometry. The prepared compounds (**1–5, 1a**–**5a**, **1b**–**5b** and **1c**–**5c**) were evaluated for antibacterial and antifungal activities against pathogenic microorganisms. The results show that the antimicrobial activity of the synthesized compounds varying a degree of inhibitory effects on the growth of different tested pathogenic strains.

Keywords Crown ether · Alkali metal complexes · Silver(I) complexes · UV and fluorescence spectroscopy · Antimicrobial activity · Pathogenic microorganism

Electronic supplementary material The online version of this article (https://doi.org/10.1007/s11164-019-03741-3) contains supplementary material, which is available to authorized users.

✉ Zeliha Hayvalı
zhayvali@science.ankara.edu.tr

[1] Department of Chemistry, Faculty of Science, Ankara University, 06100 Ankara, Turkey

[2] Science and Technology Application and Research Center, Bozok University, 66200 Yozgat, Turkey

[3] Department of Field Crops, Faculty of Agriculture, Kırşehir Ahi Evran University, 40100 Kırşehir, Turkey

Introduction

Since the pioneer work of Pedersen on crown ethers, a significant number of macrocyclic crown ether compounds were synthesized [1–7]. Owing to their great molecular variety, these ligands are very quiet for selective complex formation. Especially, crown ether rings are well known complexation groups in fluoroionophores [8–12]. They possess a cavity that allows them to reach high selectivity and sensitivity in metal cation detection [8, 13–17]. Many metal cation sensors consist of a fluorophore and a receptor unit, which are either separated by a spacer group or conjugated to each other. While the photoinduced electron transfer (PET) sensors generally have fluorophore–spacer–ionophore (guest binding site) moiety, the internal charge transfer sensors (ICT) consist of a receptor is part of the π-conjugated system of the fluorophore [18]. Crown ether ligands exhibit ionophoric properties in membranes, behaving very similarly to the biologically very important ionophore groups such as valinomycin, gramicidin, nonactin, which makes crown ether compounds especially useful in chemical and biological studies, and their pharmaceutical potentials are very large [19–21]. Furthermore, these compounds, possessing additional other functional groups, have emerged as one of the most influential architectural motifs for supramolecular compounds. The combination of pyridine derivatives with benzo-15-crown-5 group results in the design of the new ditopic compounds. The 15-crown-5 group can bind with alkali metal cations in the crown ether cavity, whereas the pyridine group binds transition and heavy metal ions with the N atom of the heterocyclic pyridine group. There are many studies in the literature of Ag(I) complexes bound to the N atom of the pyridine ligand with different binding modes and coordination numbers [22–24]. Therefore, investigating the structures and properties of Ag(I)-pyridine coordination complexes would be a worthy and interesting work.

In this study, 15-crown-5 was chosen as an ionophore, and substituted pyridine derivatives act as an additional chelating moiety (Scheme 1).

We have examined the effects of changing the type and position of the electron donor or acceptor group (–CH_3, Cl, Br, and NO_2) on the pyridine ring (Scheme 2). This means that the molecular structures of 2-nitropyridine derivatives are seldom

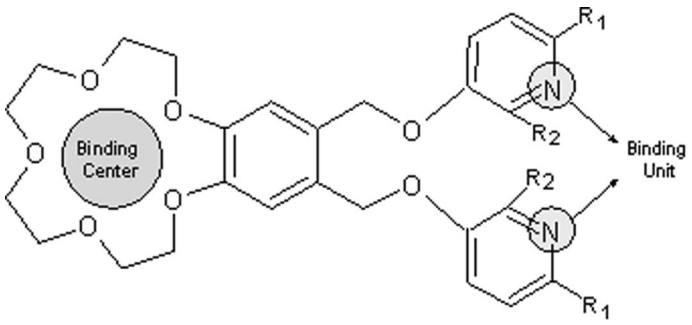

Scheme 1 Ditopic crown ether ligands

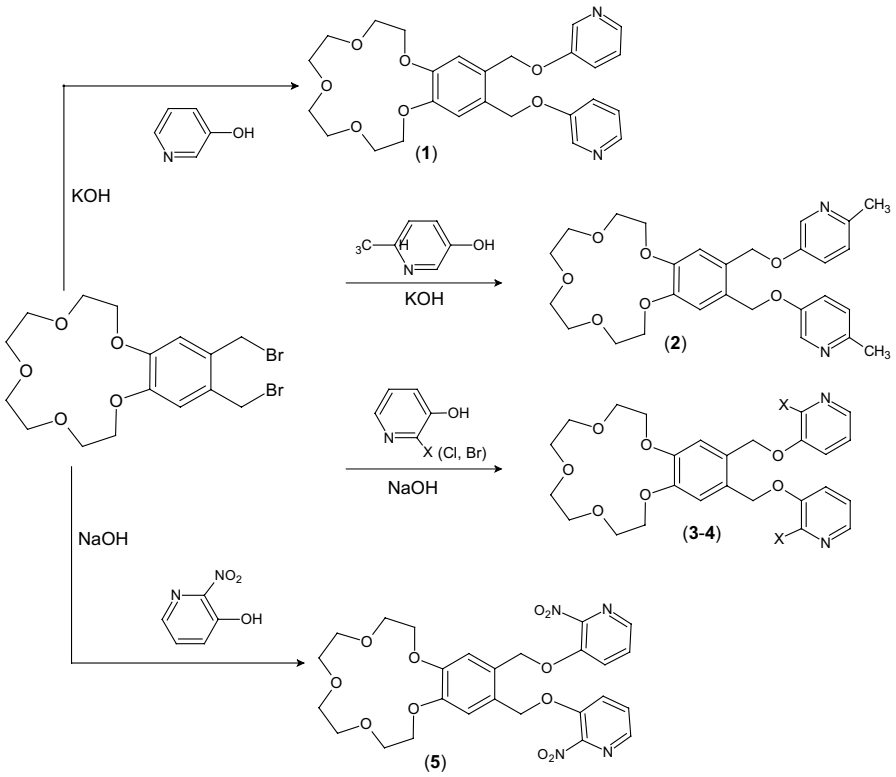

Scheme 2 Synthesis of new double-armed crown ethers (**1**–**5**)

investigated according to 3- and 4-nitropyridine [25]. 3-Benzyloxy-2-nitropyridine compound is an important intermediate for the synthesis of asymmetric cyanine dyes for the fluorescence detection of nucleic acids [25, 26]. 2-Chloropyridine derivatives are key synthetic intermediates for many pharmaceutical and commercially relevant products [27–29].

The 4′,5′-bis(bromomethyl)benzo-15-crown-5 and 3-hydroxy pyridine and derivatives were used as starting materials, and a series of new double-armed crown ether compounds were prepared (**1**–**5**) (Scheme 2). The sodium (**1a**–**5a**), potassium (**1b**–**5b**) and silver(I) complexes (**1c**–**5c**) were prepared by the reactions of new ligands (**1**–**5**) with metal salts (Scheme 3). In this paper, we suggest new ditopic ligands (**1**–**5**) in which pyridine groups are able to coordinate transition metal ion (Ag^+), while the 15-crown-5 moiety binds with alkali metal ions (Na^+ and K^+). All of the new crown ether compounds are described, and their IR, mass, ^{1}H- and ^{13}C-NMR spectral data are reported.

The complex compositions of different metal cations (Na^+, Li^+, K^+, Fe^{3+}, Cu^{2+}, Ca^{2+}, Ba^{2+} and Al^{3+}) with the ligands (**1**–**5**) were determined by using absorption and fluorescence study in EtOH. Because it was known that crown ether ligands could bind metal cations, we were motivated to test the existence

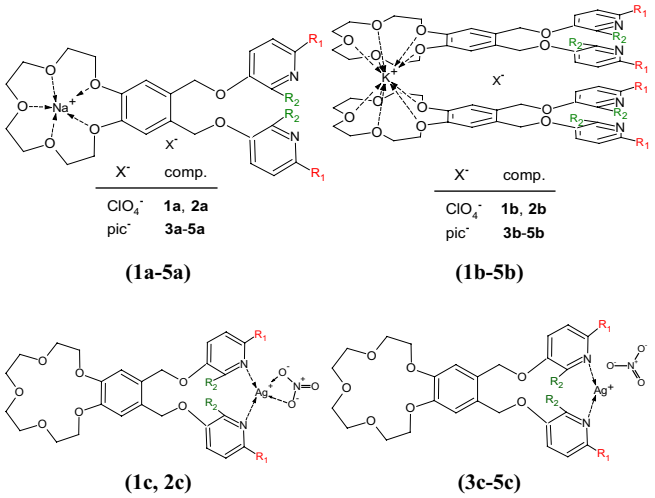

Comp.	R_1	R_2
1a, **1b**, **1c**	H	H
2a, **2b**, **2c**	CH_3	H
3a, **3b**, **3c**	H	Cl
4a, **4b**, **4c**	H	Br
5a, **5b**, **5c**	H	NO_2

Scheme 3 Synthesized sodium (**1a**–**5a**), potassium (**1b**–**5b**) and silver(I) (**1c**–**5c**) complexes

of metal ions by reviewing the changes of fluorescence intensity of new ligands (**1**–**5**). The variants of the emission spectra of this ditopic receptor detected upon different metal ion addition make the ligand convenient for multitasking sensors. Double-armed crown ethers are composed of two flexible side arm provides further coordination of a guest cation trapped in a crown ether ring and side arms. So, multiple binding sites (crown ether group and side arms) are stronger cation binders in comparison to ordinary crown ethers, they offer great promise in the area metal sensing and design of smart fluorescence-based sensor processes [30, 31].

New crown ether ligands and complexes were investigated for antimicrobial activity against pathogenic strains; *Staphylococcus aureus*, *Listeria monocytogenes* 4b, *Escherichia coli*, *Salmonella typhi H*, *Staphylococcus epidermis*, *Micrococcus luteus*, *Bacillus cereus* and antifungal activity against *Candida albicans*.

Experimental

Reagents and equipments

The starting chemicals, tetraethylene glycol dichloride [32], benzo-15-crown-5 [1] and 4′,5′-bis(bromomethyl)benzo-15-crown-5 [33] were prepared according to the cited literature. All solvents and pyridine derivatives (3-hydroxypyridine, 3-hydroxy-6-methylpyridine, 3-hydroxy-2-chloropyridine, 3-hydroxy-2-bromopyridine and 3-hydroxy-2-nitropyridine) were purchased from Sigma-Aldrich Chemical Company and used without any further purification. Alkali metal picrates were prepared according to the literature method [34]. Perchlorate and picrate salts of metal complexes with organic ligands are potentially explosive. All of the solvents

were used without further purification. Melting points were controlled on a Gallenkamp melting point platform. ^{1}H NMR spectra were detected on a VARIAN Mercury 400 MHz spectrometer. ^{1}H NMR chemical shifts (δ) are given in ppm downfield from Me_4Si, determined by chloroform ($\delta = 7.26$ ppm).^{13}C NMR spectra were detected on a VARIAN Mercury 400 MHz spectrometer. ^{13}C NMR chemical shifts (δ) are reported in ppm with the internal $CDCl_3$ at δ 77.0 ppm as standard. IR spectra were recorded on a Shimadzu Infinity FTIR spectrometer and were reported in cm^{-1} units. Mass spectral analyses were performed on an Agilent Technologies 6224 TOF LC/MS spectrometer. UV–visible spectra were recorded on a HITACHI u2800 UV–Vis spectrophotometer. Fluorescence spectra were recorded on a Perkin Elmer LS 50 B Fluorescence Spectrometer.

Test microorganisms

The pathogenic bacterial cultures chosen were; *Staphylococcus aureus* ATCC25923, *Escherichia coli* ATCC1280, *Salmonella typhi* H NCTC901.8394, *Staphylococcus epidermis* ATCC12228, *Micrococcus luteus* ATCC9341, *Bacillus cereus RSKK-863*, *Listeria monocytogenes* 4b ATCC19115 and yeast were used *Candida albicans* Y-1200-NIH.

Detection of antimicrobial activity

The synthesized compounds (**1–5, 1a–5a, 1b–5b and 1c–5c**) were examined for their antimicrobial activity by the well diffusion method against five Gram-positive bacteria (*S. aureus*, *S. epidermis*, *M. luteus*, *B. cereus*, *L. monocytogenes* 4b) and two Gram-negative bacteria (*S. typhi H*, *E. coli* and yeast *C. albicans*). A variety of laboratory methods can be used to evaluate or screen the in vitro antimicrobial activity of a pure compound [35–44]. The well diffusion method was applied for the detection of antimicrobial activity.

All compounds were maintained dry at room temperature and dissolved (10^3 µM) in DMSO. DMSO was found to have no antimicrobial activity against any of the tested organisms. 1% (v/v) of 24 h broth culture (pathogenic microorganisms) containing 10^6 CFU/mL was placed in sterile petri dishes. Mueller–Hinton Agar (MHA) (15 mL) kept at 45 °C was then poured into the petri dishes and allowed to solidity. Then wells of 6 mm diameter were punched carefully by using a sterile cork borer and were entirely filled with the synthesized compounds. The plates were incubated for 24 h at 37 °C. At the end of the incubation period, the mean value obtained for the two wells was used to calculate the zone of growth inhibition of each sample [45–47]. Pathogenic bacterial cultures and yeast were tested for resistance to five antibiotics produced by Oxoid Lt., Basingstoke, UK. These were: ampicillin (prevents the growth of Gram-negative bacteria), nystatin (binds to sterols in the fungal cellular membrane and alters the permeability allowing leakage of the cellular contents), kanamycin (used in molecular biology as an agent in isolating bacteria), sulphamethoxazole (a bacteriostatic antibacterial agent that interferes with folic acid

synthesis in susceptible bacteria), amoxicillin (aβ-lactam antibiotic used to treat bacterial infections caused by sensitive microorganisms) [48, 49].

Synthesis of the compounds

General procedure for the synthesis of new crown ether ligands (1–5)

The hydroxy-pyridine derivative (1.76 mmol) was dissolved in 5 mL DMF. Then, KOH (99 mg, 17.60 mmol) was added and the reaction mixture was stirred for 1 h. Subsequently, 4′,5′-bis(bromomethyl)benzo-15-crown-5 (400 mg, 0.88 mmol) in 5 mL DMF was added small portions to the solution. The reaction mixture was refluxed for 6 h, and the consumption of the starting material has been monitored using TLC (silica, eluent; THF). Then, the oily product was extracted from the solution CH_2Cl_2:water (1:1) and was recrystallized from *n*-hexane.

General procedure for the synthesis of sodium complexes (1a, 2a)

The corresponding crown ether (**1** and **2**) (1.44 mmol) and $NaClO_4$ (176 mg, 1.44 mmol) were dissolved in EtOH (10 mL) and refluxed for 2 h. The crude complex was filtered and recrystallized from ethanol.

General procedure for the synthesis of sodium complexes (3a–5a)

The corresponding crown ether (**3**–**5**) (1.44 mmol) and sodium picrate (361 mg, 1.44 mmol) were dissolved in EtOH (10 mL) and refluxed for 2 h. The crude complex was filtered and recrystallized from ethanol.

General procedure for the synthesis of potassium complexes (1b, 2b)

The corresponding crown ether (**1**, **2**) (1.44 mmol) and KI (120 mg, 0.72 mmol) were dissolved in EtOH (10 mL) and refluxed for 2 h. The crude complex was filtered and recrystallized from ethanol.

General procedure for the synthesis of potassium complexes (3a–5a)

The corresponding crown ether (**3**–**5**) (1.44 mmol) and potassium picrate (192 mg, 0.72 mmol) was dissolved in EtOH (10 mL) and refluxed for 2 h. The crude complex was filtered and recrystallized from ethanol.

General procedure for the synthesis of silver (I) complexes (1c–5c)

The corresponding crown ether (**1**–**5**) (1.00 mmol) and $AgNO_3$ (170 mg, 1.00 mmol) were dissolved in EtOH (10 mL) and mixed at room temperature for overnight. Then diethyl ether was added and the solution was mixed at the room temperature around 1 h. The crude complex was filtered and recrystallized from CH_2Cl_2.

Results and discussion

Syntheses and structural characterisations

The new crown ether ligands (**1**–**5**) were successfully synthesized with the yield of 64%, 71%, 63%, 59% and 72%, respectively. Physical characterizations and experimental details of the ligands (**1**–**5**) and complexes (**1a**–**5a**, **1b**–**5b** and **1c**–**5c**) were given in Table S1.

The sodium complexes (**1a**–**5a**) were synthesized by using a solution of the ligand in EtOH with $NaClO_4$ (for **1a**, **2a**) or sodium picrate (for **3a**–**5a**) salts. The potassium complexes (**1b**–**5b**) were prepared by treating a solution of the ligand in EtOH with KI (for **1b**, **2b**) or potassium picrate (for **3b**–**5b**) salts. The spectroscopic results show that the stoichiometry of the sodium complexes (**1a**–**5a**) formed between Na^+:benzo-15-crown-5 was 1:1 (M:L). Because, Na^+ ion is the best fit cation for the 15-crown-5 macrocycle [50]. In the case of potassium complexes, the sandwich complexes (**1b**–**5b**) were formed between K^+ ion with the benzo-15-crown-5 unit and the stoichiometry was 1:2 (M:L) [51]. The Ag(I) complexes (**1c**–**5c**) were obtained in moderate yields by using one equivalent $AgNO_3$ salt and one equivalent new crown ether ligand in EtOH. The Ag(I) ion is of great interest in the synthesis of coordination chemistry. This is due to the flexibility of the coordination sphere, the variety of coordination numbers (2–4, rarely 5 or 6) and geometry for the Ag(I) ion [52]. The Ag(I) binding properties of heteroditopic receptors **1**–**5** might be strongly dependent on the interactional behaviours of the substituent on the pyridine ring position. Compound **2** containing -CH_3 group in the pyridine ring at position 5 while compounds **3**, **4** and **5** containing Cl, Br and NO_2 in pyridine ring, respectively, at position 1 (Scheme 4) so Ag(I) complexes were obtained different geometry. While Ag(I) can be obtained tetrahedrally coordinated in compounds 1 and 2, it forms a linear coordinated in compounds **3**–**5**. The nitrate anion serves as a chelate ligand to the Ag(I) center for complexes **1c** and **2c**. In these complexes **(1c** and **2c)**, the silver center can be coordinated by two pyridine groups, while the nitrate ions play the role another ligand with two oxygen atoms. Similar bonding modes have been observed previously [52]. The linear complexes **3c**–**5c** were prepared from two pyridine N atom with silver(I) ion. The mass spectra confirmed these assumptions.

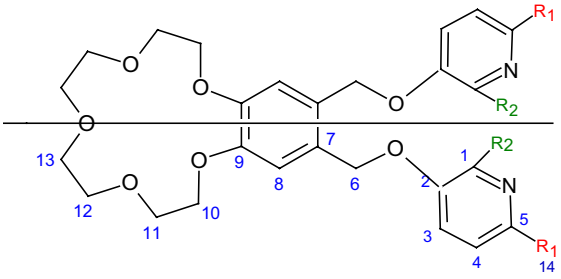

Compound	R_1	R_2
(**1**)	H	H
(**2**)	CH_3	H
(**3**)	H	Cl
(**4**)	H	Br
(**5**)	H	NO_2

Scheme 4 Numbering scheme of ligands (**1**–**5**)

All crown ether ligands (**1**–**5**) and complexes (**1a**–**5a**, **1b**–**5b** and **1c**–**5c**) were stable in solution and the structures have been identified by FT-IR, ^{1}H-NMR, ^{13}C-NMR and mass spectra. In particular, HRMS and NMR spectral results provided evidence for the formation and coordination of complexes.

FT-IR spectra

The assignments along with the vibrational frequencies of new ligands (**1**-**5**) and complexes (**1a**–**5a, 1b**–**5b** and **1c**–**5c**) are given in Table S2. IR spectra of the ligands (**1**–**5**) show a broad band at 1281; 1202 and 1121; 1053 cm^{-1} for C–O–C aromatic and C–O–C aliphatic crown ether stretching vibrations, respectively. In particular, the peaks of the C–H aliphatic bond vibrations at 2945–2864 cm^{-1} and the peaks of the aromatic C–C, C=C and C=N vibrations in the range of 1603–1344 cm^{-1} were evaluated for the ligands. The bands at about 1603–1566 cm^{-1} and 1381–1344 cm^{-1} stems from the stretching vibrations of the skeleton C=N, which belongs to the pyridine group. These peaks have also supported the structures. In the IR spectrum **5**, the asymmetric stretching ν_{as}(N=O) vibrations with strong intensity is located at 1526 cm^{-1}. The C–Cl stretching frequency is generally observed in the region 800–550 cm^{-1} [53, 54]. The IR band observed at 786 cm^{-1} has been assigned to C–Cl stretching mode for compound **3**. Three peaks were detected at approximately 990, 875 and 935 cm^{-1} in the spectra of compound **1**–**5**, respectively. The first two peaks were not detected in the spectra of the sodium and potassium complexes confirming conformational changes during a complexation event [55]. But three peaks were observed in the spectra of the Ag(I) complexes (**1c**–**5c**). These results suggest that the complexation with Ag(I) cation can be formed by the aromatic side arms of the crown ether ring. The IR spectra of **1c** and **2c** show the characteristic vibrations of N–O of coordinated nitrate groups at 1479 and 1492 cm^{-1}, respectively.

NMR spectra

The structures of the crown ether ligands (**1**–**5**), sodium (**1a**–**5a**), potassium (**1b**–**5b**) and silver(I) (**1c**–**5c**) complexes in solution were confirmed by ^{1}H-NMR spectra (see Supporting Information). The ^{1}H-NMR spectral data are summarized in Table 1. The ^{1}H-NMR spectra and the integral ratio of the aliphatic and aromatic proton peak for the ligands (**1**–**5**) and alkali metal complexes (**1a**–**5a** and **1b**–**5b**) indicates that the molecules are symmetric (Scheme 4). The signals for aliphatic methylene protons of crown ether ligands (**1**–**5**) integrated to three multiple peak groups were observed approximately at 3.73–4.18 ppm. The $-CH_2$ protons for compounds (**1**–**5**) were detected as a singlet at $\delta = 5.11$, 5.09, 5.24, 5.25 and 5.30 ppm, respectively. The $-CH_3$ proton peak for compound **2** was observed at $\delta = 2.52$ ppm. The signal for H8 proton peaks was seen as a singlet at $\delta = 7.00$, 6.99, 7.04, 7.07 and 7.04 ppm in 1–5, respectively. The multiple signals observed approximately at 7.09–8.36 ppm were attributed to the aromatic pyridine protons.

The ^{1}H-NMR spectra of the sodium and potassium complexes (**1a**–**5a** and **1b**–**5b**) are very similar to the corresponding ligand (**1**–**5**), spectra. However, the ^{1}H-NMR

Table 1 ^{1}H-NMR spectral data of ligands (**1**–**5**) (δ, ppm) (in $CDCl_3$) (proton numbers are given in Scheme 4)

Compounds	H1	H3	H4	H5	H6	H8	H10	H11	H12, H13	H14
(**1**)	8.36 (d; 2H) $^{3}J_{3\text{-}1}$: 2.4 Hz	7.20 (m; 4H)		8.23 (dd; 2H) $^{2}J_{4\text{-}5}$: 4.3 Hz $^{3}J_{3\text{-}5}$: 2.0 Hz	5.11 (s; 4H)	7.00 (s; 2H)	4.15 (t; 4H)	3.90 (t; 4H)	3.75 (t; 8H)	–
(**2**)	8.30 (d; 2H) $^{3}J_{3\text{-}1}$: 2.0 Hz	7.20 (dd; 2H) $^{2}J_{4\text{-}3}$: 8.6 Hz $^{3}J_{1\text{-}3}$: 2.0 Hz	7.09 (d; 2H) $^{2}J_{3\text{-}4}$: 8.6 Hz	–	5.09 (s; 4H)	6.99 (s; 2H)	4.15 (t; 4H)	3.90 (t; 4H)	3.75 (t; 8H)	2.52 (s; 6H)
(**3**)	–	7.31 (d; 2H) $^{2}J_{4\text{-}3}$: 8.0 Hz	7.17 (dd; 2H) $^{2}J_{5\text{-}4}$: 4.7 Hz $^{2}J_{3\text{-}4}$: 8.0 Hz	7.98 (dd; 2H) $^{2}J_{4\text{-}5}$: 4.7 Hz $^{3}J_{3\text{-}5}$: 1.2 Hz	5.24 (s; 4H)	7.04 (s; 2H)	4.10 (m; 4H)	3.87 (m; 4H)	3.73 (m; 8H)	–
(**4**)	–	7.28 (m; 2H)	7.20 (dd; 2H) $^{2}J_{5\text{-}4}$: 4.7 Hz $^{2}J_{3\text{-}4}$: 7.8 Hz	7.97 (dd; 2H) $^{2}J_{4\text{-}5}$: 4.7 Hz $^{3}J_{3\text{-}5}$: 1.2 Hz	5.25 (s; 4H)	7.07 (s; 2H)	4.11 (m; 4H)	3.87 (m; 4H)	3.74 (m; 8H)	–
(**5**)	–	7.67 (d; 2H) $^{2}J_{4\text{-}3}$: 8.3 Hz	7.55 (dd; 2H) $^{2}J_{5\text{-}4}$: 4.6 Hz $^{2}J_{3\text{-}4}$: 8.3 Hz	8.10 (dd; 2H) $^{2}J_{4\text{-}5}$: 4.6 Hz $^{3}J_{3\text{-}5}$: 1.2 Hz	5.30 (s; 4H)	7.04 (s; 2H)	4.18 (t; 4H)	3.91 (t; 4H)	3.75 (t; 8H)	–

s :singlet, *d* doublet, *t* triplet, *dd* doublet of doublets, *m* multiplet

spectra of sodium and potassium complexes provide an explicit evidence for ligands and their sodium and potassium complexes [55–57]. The small chemical shifts are more pronounced for the methylene protons of the crown ether signals (Table 2). In addition, three different multiple peaks for the ligands (**1**–**5**) were observed in the peak region of the crown ether protons (OCH_2–CH_2O), while four multiple peaks for the sodium complexes (**1a**–**5a**) and wide multiple peaks for the potassium complexes (**1b**–**5b**) (Fig. 1).

The different appearance of four signals in ^{1}H-NMR spectra of complexes (**1a**–**5a**) may point out the extent of encapsulation of the sodium cation by the crown ether cavity. The extent of cation encapsulation in the cavity of the crown ether changes the conformation of the segments bearing crown ether protons. The cationic diameter of the Na^+ ion fits well with the size of the cavity of the 15-crown-5 moiety and is expected to be attached inside the cavity, surrounded by the etheric oxygen. However, the K^+ cation is larger than the 15-crown-5 cavity and is preferred form sandwich complex composition [58–60].

In ^{1}H-NMR spectra of Ag(I) complexes (**1c**–**5c**), the shifts in the peaks of aromatic protons in the pyridine ring are more distinct (Table 3). For example, H3 and H4 proton peaks were detected at 7.18 and 7.08 ppm as a multiplet for compound **2**, same proton peaks were detected at 7.39 and 7.20 ppm as a quartet and doublet for complex **2c**. Similar changes have been observed for complexes **3c**–**5c**. The $–CH_3$ protons (H14) peak for complex **2c** was observed at 2.40 ppm. This proton peak was observed at a chemical shift of 12 ppm lower than the free ligand. The aliphatic $–CH_2$ (H6) and aromatic H8 protons were observed as singlet peaks with small shifts compared to the ligand. As a result, the binding of the Ag(I) ion to the pyridine N atom results in a more pronounced effect on the electronic structure of the pyridine protons, thereby significant shifts in pyridine proton signals while the crown ether methylene proton signals remain unchanged (Fig. 1).

The ^{13}C-NMR spectral data for ligands (**1**–**5**) were given in Table S3. The spectra indicate that the molecules are symmetric (Scheme 4). Therefore, in the ^{13}C-NMR (decoupled) spectra of the ligands (**1**–**5**) four crown ether carbons (C_{10}–C_{13}) were observed between 67.43 and 71.02 ppm. The $–CH_3$ carbon (C14) peak in **2** was observed at 23.30 ppm. Aliphatic $–CH_2$ carbons (C6) for compounds **1**–**5** were detected in crown ether carbons peak region at 68.04, 68.24, 68.66, 68.70 and 69.14 ppm, respectively. In addition, other aromatic carbon peaks were detected in the expected region and expected numbers. The ^{13}C-NMR spectra of the sodium, potassium and silver(I) complexes (**1a**–**5a**, **1b**–**5b** and **1c**–**5c**) are very similar to the corresponding ligand (**1**–**5**) spectra (Table S4).

Ms spectra

We have reported that HRMS is a powerful tool in the determination of structures of new double armed benzo-15-crown-5 ligands (**1**–**5**), sodium (**1a**–**5a**), potassium (**1b**–**5b**) and silver(I) complexes (**1c**–**5c**). In keeping with this, the structures of the ligands and complexes in CH_3CN solution were examined by HRMS at 298 K. Only single isotope mass spectra are presented in which the most intense

Table 2 ^{1}H-NMR spectral data of sodium and potassium complexes (**1a–5a**, **1b–5b**) (δ, ppm)

Compounds	H1	H3	H4	H5	H6	H8	H10	H11	H12	H13	H14
(**1a**)[a]	8.36 (t; 2H)	7.23 (m; 4H)		8.25 (m; 2H)	5.12 (s; 4H)	7.06 (s; 2H)	4.25 (t; 4H)	3.95 (t; 4H)	3.73 (t; 4H)	3.81 (t; 4H)	–
	$^{3}J_{3\text{-}1}$: 1.8 Hz										
(**2a**)[a]	8.21 (d; 2H)	7.14 (dd; 2H)	7.06 (d; 2H)	–	5.07 (s; 4H)	7.04 (s; 2H)	4.23 (t; 4H)	3.94 (t; 4H)	3.72 (t; 4H)	3.79 (t; 4H)	2.52 (s; 12H)
	$^{3}J_{3\text{-}1}$: 2.8 Hz	$^{2}J_{4\text{-}3}$: 8.5 Hz	$^{2}J_{3\text{-}4}$: 8.5 Hz								
		$^{3}J_{1\text{-}3}$: 2.8 Hz									
(**3a**)[a]	–	7.28–7.31 (dd; 2H)	7.17–7.20 (dd; 2H)	7.99–8.00 (dd; 2H)	5.21 (s; 4H)	7.06 (s; 2H)	4.14 (m; 4H)	3.96 (m; 4H)	3.77 (m; 4H)	3.81 (m; 4H)	–
		$^{2}J_{4\text{-}3}$: 8.1 Hz	$^{2}J_{5\text{-}4}$: 4.6 Hz	$^{2}J_{4\text{-}5}$: 4.6 Hz							
		$^{3}J_{5\text{-}3}$: 1.3 Hz	$^{2}J_{3\text{-}4}$: 8.1 Hz	$^{3}J_{3\text{-}5}$: 1.3 Hz							
(**4a**)[b]	–	7.62 (dd; 2H)	7.40 (dd; 2H)	7.95 (dd; 2H)	5.33 (s; 4H)	7.22 (s; 2H)	4.09 (t; 4H)	3.77 (t; 4H)	3.61 (m; 8H)		–
		$^{2}J_{4\text{-}3}$: 8.1 Hz	$^{2}J_{5\text{-}4}$: 4.5 Hz	$^{2}J_{4\text{-}5}$: 4.5 Hz							
		$^{3}J_{5\text{-}3}$: 1.5 Hz	$^{2}J_{3\text{-}4}$: 8.1 Hz	$^{3}J_{3\text{-}5}$: 1.5 Hz							
(**5a**)[a]	–	7.70 (d; 2H)	7.59 (dd; 2H)	8.13 (dd; 2H)	5.30 (s; 4H)	7.12 (s; 2H)	4.27 (m; 4H)	4.04 (m; 4H)	3.80 (t; 4H)	3.83 (t; 4H)	–
		$^{2}J_{4\text{-}3}$: 8.5 Hz	$^{2}J_{5\text{-}4}$: 4.4 Hz	$^{2}J_{4\text{-}5}$: 4.4 Hz							
			$^{2}J_{3\text{-}4}$: 8.5 Hz	$^{3}J_{3\text{-}5}$:1.2 Hz							
(**1b**)[a]	8.28 (d; 2H)	7.27 (m; 4H)	7.19 (dd; 4H)	8.18 (dd; 4H)	5.14 (s; 8H)	6.92 (s; 4H)	3.74 (m; 32H)				–
	$^{3}J_{3\text{-}1}$: 3.1 Hz		$^{2}J_{3\text{-}4}$: 8.4 Hz	$^{2}J_{4\text{-}5}$: 4.5 Hz							
			$^{2}J_{5\text{-}4}$: 4.5 Hz	$^{3}J_{3\text{-}5}$: 1.4 Hz							
(**2b**)[b]	8.16 (d; 2H)	7.31 (dd; 4H)	7.12 (m; 4H)	–	5.13 (s; 8H)	7.11 (s; 4H)	4.04 (t; 8H)	3.71 (t; 8H)	3.57 (m; 8H)	3.59 (m; 8H)	2.35 (s; 12H)
	$^{3}J_{3\text{-}1}$: 3.1 Hz	$^{2}J_{4\text{-}3}$: 8.6 Hz	$^{2}J_{3\text{-}4}$: 8.6 Hz								
		$^{3}J_{1\text{-}3}$: 3.1 Hz									

Table 2 (continued)

Compounds	H1	H3	H4	H5	H6	H8	H10	H11	H12	H13	H14
(**3b**)[a]	–	7.28 (m; 4H)	7.16 (dd; 4H)	7.97 (dd; 4H)	5.20 (s; 8H)	6.98 (s; 4H)	3.99 (m; 8H)	3.83 (m; 8H)	3.72 (m; 8H)	3.76 (m; 8H)	–
			$^{2}J_{5\text{-}4}$: 4.7 Hz	$^{2}J_{4\text{-}5}$: 4.7 Hz							
			$^{2}J_{3\text{-}4}$: 8.2 Hz	$^{3}J_{3\text{-}5}$: 1.2 Hz							
(**4b**)[b]	–	7.60 (dd; 4H)	7.39 (dd; 4H)	7.95 (dd; 4H)	5.32 (s; 8H)	7.22 (s; 4H)	4.08 (t; 8H)	3.76 (t; 8H)	3.59 (m; 8H)	3.61 (m; 8H)	–
		$^{2}J_{4\text{-}3}$: 8.2 Hz	$^{2}J_{5\text{-}4}$: 4.6 Hz	$^{2}J_{4\text{-}5}$: 4.6 Hz							
		$^{3}J_{5\text{-}3}$: 1.3 Hz	$^{2}J_{3\text{-}4}$: 8.2 Hz	$^{3}J_{3\text{-}5}$: 1.3 Hz							
(**5b**)[a]	–	7.81 (m; 4H)	7.58 (dd; 4H)	8.10 (d; 4H)	5.35 (s; 8H)	7.02 (s; 4H)	3.76 (m; 32H)				–
			$^{2}J_{5\text{-}4}$: 4.2 Hz	$^{2}J_{4\text{-}5}$: 4.2 Hz							
			$^{2}J_{3\text{-}4}$: 8.4 Hz								

s singlet, *d* doublet, *t* triplet, *dd* doublet of doublets, *m* multiplet

[a]In $CDCl_3$

[b]In DMSO-d_6

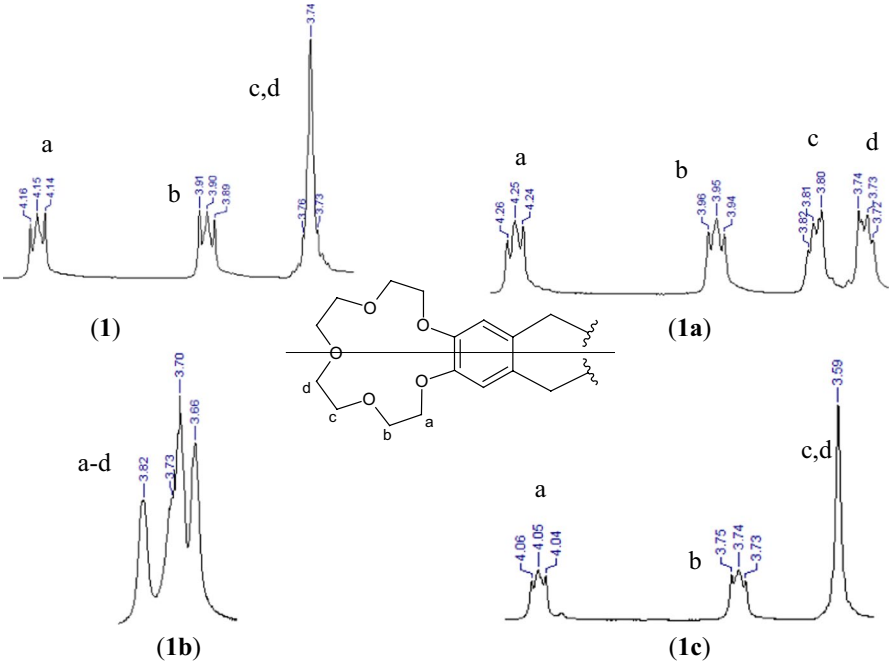

Fig. 1 ^{1}H-NMR spectra of the crown ether protons [ligand (**1**); sodium complex (**1a**); potassium complex (**1b**); silver(I) complex (**1c**)] (in $CDCl_3$)

peak in the pattern was selected and intensities of molecular ion peaks (found and calculated) and error ratios (ppm) of the compounds are summarized in Table 4. The isotope peaks pattern of the compounds (**3, 4**, **3a, 4a, 3b, 4b** and **1c**–**5c**) are given as a detailed list in Table 5. High-resolution MS can replace elemental analysis for chemical formula confirmation. Compound (**1**) spectrum show that the molecular ion peak $[M+H]^+$ at *m*/*z* 483.2146. In the mass spectra of other ligands (**2**–**5**) the dominant peak at *m*/*z* 533.22467, 573.11581, 663.01264 and 595.16423, respectively corresponds to the ligand plus sodium $[M+Na]^+$. In addition, $[M+K]^+$ peaks were observed in these spectra (It is very common to see Na and K adducts in the HRMS-TOF spectra) (Fig. S1).

In the mass spectra of sodium complexes (**1a**–**5a**), the molecular ion peaks corresponds to the ligand plus sodium ($[M+Na]^+$). The sodium cation is bound by the ion–dipole interaction to the crown ether cavity. The molecular ion peak $[2M+K]^+$ were detected at *m*/*z* 1003.37051, 1059.43612, 1141.21083, 1319.00369 and 1183.30812 for the other potassium complexes (**1b**–**5b**), respectively. These peaks are corresponding to the 1:2 (metal:ligand) complexes. In this work, the elements giving rise to significant M + 2 and M + 4 peaks are chlorine and bromine. A ratio of M to M + 2 and M + 4 of approximately 9:6:1 (for chlorine) and 1:2:1 (for bromine) indicates the presence of a two chlorine and bromine in compounds (**3**, **4**, **3a**, **4a**, **3b** and **4b**) (Fig. S1).

Table 3 ^{1}H-NMR spectral data of silver(I) complexes (**1c–5c**) (δ, ppm)

Compounds	H1	H3	H4	H5	H6	H8	H10	H11	H12	H13	H14
(**1c**)[b]	8.31 (d; 2H)	7.45 (m; 2H)	7.31 (dd; 2H)	8.14 (dd; 2H)	5.18 (s; 4H)	7.14 (s; 2H)	4.05 (t; 4H)	3.74 (t; 4H)	3.59 (m; 4H)		
	$^{3}J_{3\text{-}1}$: 2.7 Hz		$^{2}J_{3\text{-}4}$: 8.6 Hz	$^{2}J_{4\text{-}5}$: 4.7 Hz							
			$^{2}J_{5\text{-}4}$: 4.7 Hz	$^{3}J_{3\text{-}5}$: 1.2 Hz							
(**2c**)[b]	8.18 (d; 2H)	7.41 (dd; 2H)	7.21 (d; 2H)	–	5.14 (s; 4H)	7.11 (s; 2H)	4.04 (t; 4H)	3.74 (t; 4H)	3.80 (m; 4H)		2.40 (s; 6H)
	$^{3}J_{3\text{-}1}$: 3.1 Hz	$^{2}J_{4\text{-}3}$: 8.6 Hz	$^{2}J_{3\text{-}4}$: 8.6 Hz								
		$^{3}J_{1\text{-}3}$: 3.1 Hz									
(**3c**)[a]	–	7.28–7.30 (m; 2H)	7.23 (m; 2H)	8.00 (dd; 2H)	5.24 (s;4H)	7.05 (s; 2H)	4.07 (m; 4H)	3.86 (m; 4H)	3.75 (m; 8H)		
				$^{2}J_{4\text{-}5}$: 4.5 Hz							
				$^{3}J_{3\text{-}5}$: 1.4 Hz							
(**4c**)[a]	–	7.31–7.34 (m; 2H)	7.18–7.21 (m; 2H)	7.99–8.00 (dd; 2H)	5.23 (s;4H)	7.01 (m; 2H)	4.08 (m; 4H)	3.86 (m; 4H)	3.74 (m; 8H)		
				$^{2}J_{4\text{-}5}$: 4.7 Hz							
				$^{3}J_{3\text{-}5}$: 1.2 Hz							
(**5c**)[a]	–	7.66 (d; 2H)	7.55 (m; 2H)	8.11 (d; 2H)	5.29 (s; 4H)	7.04 (s; 2H)	4.18 (t; 4H)	3.92 (t; 4H)	3.75 (m; 8H)		
		$^{2}J_{4\text{-}3}$: 7.8 Hz		$^{2}J_{4\text{-}5}$: 4.3 Hz							

s singlet, *d* doublet, *t* triplet, *dd* doublet of doublets, *m* multiplet

[a]In $CDCl_3$

[b]In DMSO-d_6

Table 4 Mass spectral data (in CH_3CN)

Compounds	Molecular ion peak	Mass (found g/mol)	Mass (calculated g/mol)	Error ratio (ppm)
(**1**)	$[M+H]^+$	483.21465	483.21317	− 3.06
(**2**)	$[M+Na]^+$	533.22497	533.22641	− 2.70
	$[M+K]^+$	549.19952	549.20035	− 1.51
(**3**)	$[M+Na]^+$	573.11581	573.11717	2.37
	$[M+K]^+$	589.08981	589.09111	2.21
(**4**)	$[M+Na]^+$	663.01264	663.01409	2.19
	$[M+K]^+$	678.98666	678.98803	2.02
(**5**)	$[M+Na]^+$	595.16423	595.16529	1.78
(**1a**)	$[M+Na]^+$	505.19482	505.19511	0.57
(**2a**)	$[M+Na]^+$	533.22702	533.22641	− 1.14
(**3a**)	$[M+Na]^+$	573.11444	573.11717	4.76
(**4a**)	$[M+Na]^+$	663.01121	663.01409	4.34
(**5a**)	$[M+Na]^+$	595.16325	595.16529	3.43
(**1b**)	$[2M+K]^+$	1003.37051	1003.37439	3.87
(**2b**)	$[2M+K]^+$	1059.43612	1059.43699	0.82
(**3b**)	$[2M+K]^+$	1141.21083	1141.21555	4.14
(**4b**)	$[2M+K]^+$	1319.00369	1319.01234	6.58
(**5b**)	$[2M+K]^+$	1183.30812	1183.31474	5.59
(**1c**)	$[M+Ag+NO_3+Na]^+$	674.08940	674.08804	− 2.02
(**2c**)	$[M+Ag+NO_3+Na]^+$	702.12109	702.11934	− 2.49
(**3c**)	$[M+Ag]^+$	659.02913	659.02955	0.64
(**4c**)	$[M+Ag]^+$	746.92746	746.92942	2.62
(**5c**)	$[M+Ag]^+$	679.07780	679.08062	4.15

Table 5 Molecular ion peaks (related to natural abundance) (g/mol)

Compounds	[M]	[M+2]	[M+4]
(**3**)	589.08981 [M+K]	591.08756 [M+2+K]	–
(**4**)	676.98856 [M+K]	678.98666 [M+2+K]	680.98517 [M+4+K]
(**3a**)	573.11444 [M+Na]	575.11203 [M+2+Na]	–
(**4a**)	661.01377 [M+Na]	663.01121 [M+2+Na]	665.01087 [M+4+Na]
(**3b**)	1141.21083 [2M+K]	1143.20895 [2M+2 + K]	–
(**4b**)	1317.00495 [2M+K]	1319.00369 [2M+2 + K]	1321.00123 [2M+4 + K]
(**1c**)	674.08940 [M+Na+Ag+NO_3]	676.08951 [M+2 + Na+Ag+ NO_3]	–
(**2c**)	702.12109 [M+Na+Ag+NO_3]	704.12130 [M+2+Na+Ag+NO_3]	–
(**3c**)	659.02913 [M+Ag]	661.02376 [M+2+Ag]	–
(**4c**)	746.92746 [M+Ag]	748.92633 [M+2+Ag]	–
(**5c**)	679.07780 [M+Ag]	681.07887 [M+2+Ag]	–

M: Ligand

In the mass spectra of silver(I) complexes (**1c** and **2c**), the molecular ion peaks correspond to the ligand plus silver nitrate and sodium ($[M+Ag+NO_3+Na]^+$). A ratio of M and M + 2 of approximately 1:1 indicates the presence of one silver(I) ion in a complex (Tables 4, 5) (Fig. S2). The silver(I) ion is bound to the side arm of the ligand (pyridine N atom) and nitrate anion (Scheme 3). The silver(I) complexes (**3c**–**5c**), the molecular ion peaks corresponds to the ligand plus silver ($[M+Ag]^+$). In compounds **3c** and **4c**, unlike compounds **1c** and **2c**, the nitrate anion was not coordinated by the silver ion. The complexes **3c** and **4c** have the isotope peaks of the M and M + 2 from the chlorine, bromine and silver atoms (Fig. S2). The spectrum of the silver complex **5c** shows that the M and M + 2 peaks at 679.07780 and 681.07887, respectively. A ratio of the peaks is 1:1 as expected for silver(I) isotope peak patterns (Fig. S2).

Optical characteristics

Crown ether rings are well-known ionophores due to their metal binding ability. Crown ethers attached to a fluorophore group are named fluoroionophores and have a large structural variety that allows for high selectivity and sensitivity for metal ion detection. Synthesized ditopic ligands (**1**–**5**) centre hold various selectivities to metal ions, and having two binding units causes changes in the photophysical properties of the complex receptor (Scheme 1). In this case, the substantial optical changes upon complex formation can be suggested.

The UV–vis absorption and emission spectra were recorded at a concentration of 5×10^{-5} M in EtOH. The room temperature UV–vis spectra of new ligands **1**–**5** exhibited one main absorption band at around λ_{max} 292 nm (Fig S3). These peaks correspond to the $S_0 \rightarrow S_1$ transition of the benzo-15-crown-5 moieties [15]. All compounds (**1**–**5**) exhibit absorption patterns that can be assigned characteristic of benzo-crown ethers. It has been seen that binding of different substituted pyridine units to the ligand (**1**–**5**) structure weakly affects the absorption wavelength band. The close values of intensities of the absorption bands of the ligands (**1**–**4**) and a small difference in the absorption maxima positions points at identical interactions of substituted pyridine units and benzo-15-crown-5 in the ground state. The UV–vis behavior of compound **5** in the presence of the NO_2 group in pyridine it prevents the charge transfer from the donor crown ether to acceptor nitro pyridine moiety leading to a blue shift in the absorption band (Fig. S3).

The fluorescence emission spectra of ligands (**1**–**5**) in EtOH media were investigated and showed in Fig. 2. Compound **1** and **2** containing –H and $–CH_3$ substituted in the pyridine ring show the highest fluorescence intensity while compounds **3** and **4** containing –Cl and –Br substituted in pyridine ring have lowest fluorescence intensity among the synthesized ligands (**1**–**5**) (Fig. 2). As is known, the spin–orbit interaction of electronic states has a great influence on the optical properties of compounds. The presence of heavy atoms (Cl, Br) in the synthesized compounds (**3** and **4**) increases the inter-system crossing process, which causes the change in optical properties. This effect is known as the heavy atom effect. As a result, in the synthesized compounds (**1**–**5**), the fluorescence signal was increased for compounds **1** and

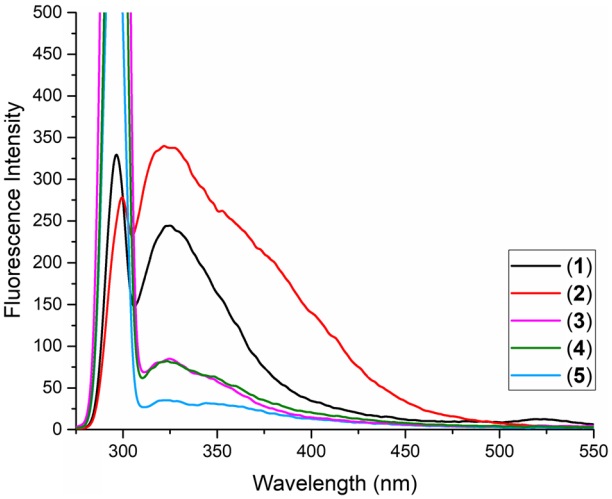

Fig. 2 The fluorescence spectra of ligands (**1**–**5**); 25 °C; λ_{exc}: 292 nm; ligand concentration *c*: 5×10^{-5} in EtOH

2 while decreasing for compounds **3** and **4** due to the intersystem crossing mechanism. The nitro group decreases the fluorescence signals due to their electron withdrawing nature [15]. In general, nitro substituted rings have a lower LUMO energy level due to the electron-withdrawing effect of the nitro group. Note that for the nitro substituted compound **5**, very weak fluorescence in the emission spectra was observed compared to the other compounds (**1**–**4**), likely related to the significant decrease of the LUMO energy level and intramolecular charge transfer state process was occurred [61, 62].

Our fluorescence investigations showed that introducing substituents (H, $–CH_3$, –Cl, –Br and $–NO_2$) on the pyridine group may affect the fluorescence intensity (Fig. 2).

To investigate the metal selectivity of synthesized ligands (**1**–**5**), different metal cations (Li^+, Na^+, K^+, Fe^{3+}, Cu^{2+}, Ca^{2+}, Ba^{2+} and Al^{3+}) were added to these ligands and fluorescence spectra were recorded (Fig. 3).

In metal selectivity studies of all synthesized ligands (**1**–**5**), different fluorescence intensities were recorded with each metal cations (Li^+, Na^+, K^+, Fe^{3+}, Cu^{2+}, Ca^{2+}, Ba^{2+} and Al^{3+}). As a common feature in all ligands (**1**–**5**) fluorescence was quenched by the addition of Fe^3 and Cu^{2+}. Meanwhile, the weak fluorescence emission was detected for five ligands (**1**–**5**), with the upon addition of Li^+, Na^+ or K^+ cations. To find the effect of joining together two ionophore units on metal cation complexation in solution, compound **1** has been chosen. The optical study of compound **1** was performed with the addition of increasing amounts of Na^+, Fe^{3+} and Cu^{2+} ions (commonly selected ions) concentration in EtOH (Fig. 4).

The ligands (**1**–**5**) that are synthesized have two different binding sites (the crown ether cavity and the pyridine N atoms) (Scheme 1). In this respect, it can be considered that the Na^+ ion complex was formed from the crown ether cavity and the

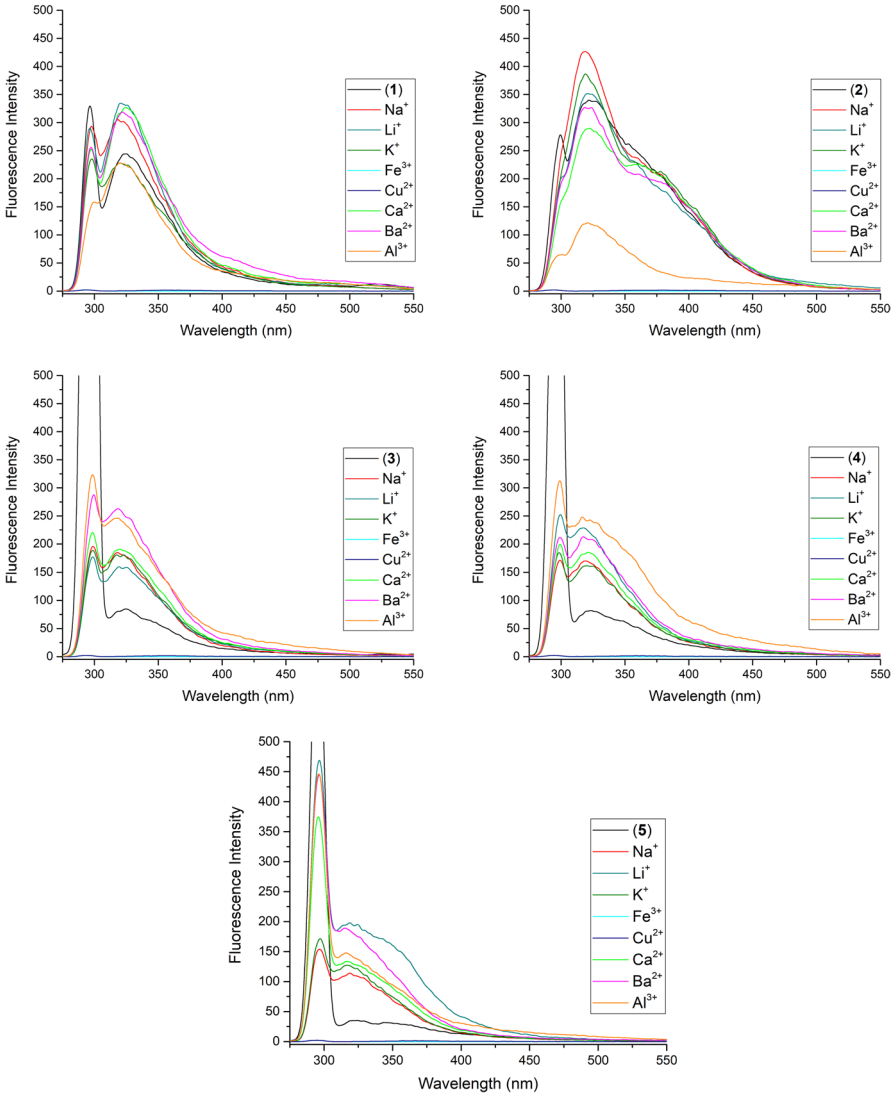

Fig. 3 The effect of metal cations on the fluorescence spectra of ligands (**1**–**5**); metal salt anions: Na^+ and K^+: I^-; others: NO_3^-; 25 °C; λ_{exc}: 292 nm; ligand concentration *c*: 5×10^{-5} metal concentrations *c*: 5×10^{-3} M in EtOH

transition metal ion (Fe^{3+} and Cu^{2+}) complexes were formed from the pyridine N atoms. In the titration study of compound **1** with three metal ions (Na^+, Fe^{3+} and Cu^{2+}), only at about 325 nm peak intensity increase (for the addition of Na^+ ion) or decrease (for the addition of Fe^{3+} or Cu^{2+} ion) was observed (Fig. 4). However, a new peak was recorded at about 430 nm in the synthesized Ag(I) complex (**1c**) (Fig. 5). This peak belongs to the complex. The lack of a new peak (at about 430 nm) in the titration studies of Fe^{3+} and Cu^{2+} ion suggests that the Fe^{3+} and Cu^{2+}

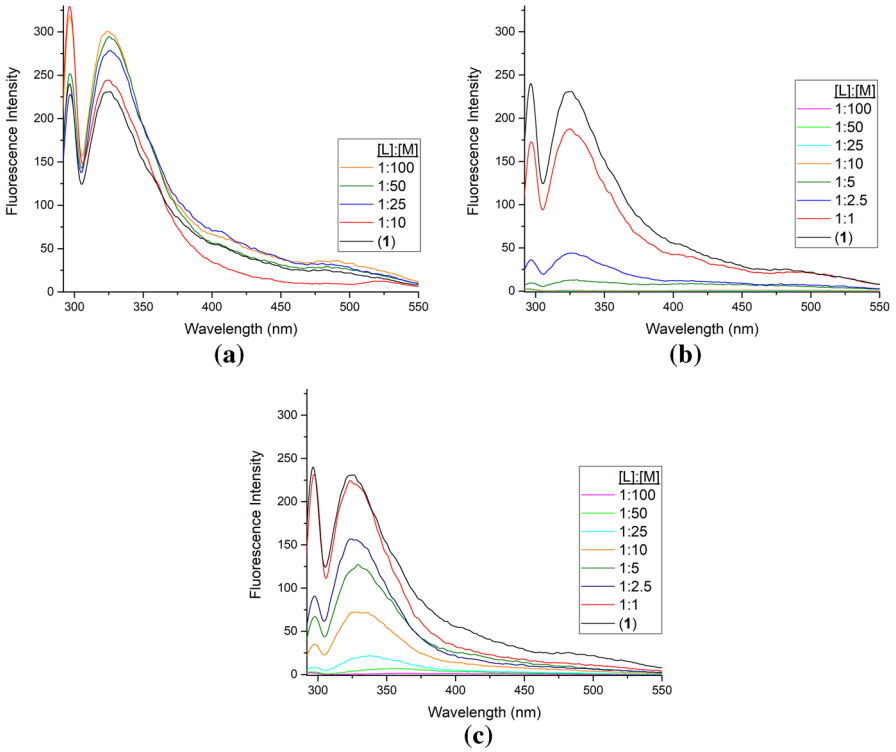

Fig. 4 The fluorescence spectral changes of compound **1** during the addition of 1–100 equivalent of **a** Na^{+}, **b** Fe^{3+}, **c** Cu^{2+}. 25 °C; λ_{exc}: 292 nm; ligand concentration *c*: 5×10^{-5} metal concentration *c*: 5×10^{-3} M in EtOH

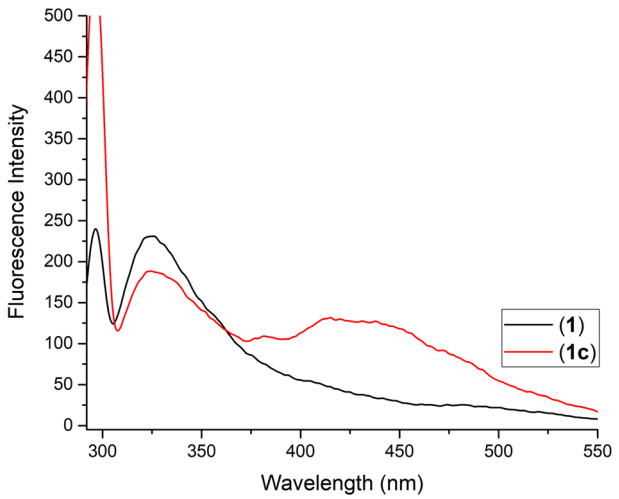

Fig. 5 The fluorescence spectrum of compound **1** and **1c** 25 °C; λ_{exc}: 292 nm; complex concentration *c*: 5×10^{-5} in EtOH

ion complexes formed may have given inclusion complexes with the crown ether ring.

In compounds **1**–**5**, pyridine group is deconjugated with benzo-15-crown-5 group and photoinduced electron transfer (PET) mechanism that may be occurred between the benzo-15-crown-5 and pyridine fragments (Scheme 5). Intramolecular PET mechanism is a well-known process through which the fluorescence of a fluorophore is quenched by electron transfer from the receptor (crown ether) to the fluorophore group [63]. In the absence of metal cation (Fe^{3+} or Cu^{2+}), the HOMO of the receptor lies lower in energy than fluorophore and prevents an electron transfer from the donor to the acceptor, so fluorescence occurred. Binding of the sensor to its metal cation (Fe^{3+} and Cu^{2+}) lowers the receptor HOMO and LUMO energy level below that of the fluorophore LUMO than that of the donor can transfer an electron to the receptor's LUMO, so fluorescence was quenched. By this reason for Fe^{3+} and Cu^{2+} complexation process was assigned oxidative-PET mechanism [63]. After coordination with alkali metal (Li^+, Na^+, K^+) cation, the electron-rich element as oxygen in crown group will be bound. Therefore, the PET action from the crown donor towards the side group is stopped and fluorescence is occurred for compounds **1**–**5**.

Antimicrobial activity

The synthesized compounds (**1**–**5, 1a**–**5a**, **1b**–**5b** and **1c**–**5c**) were screened for in vitro antibacterial and antifungal activity in DMSO as a test substance. The ligands (**1**–**5**) and complexes (**1a**–**5a**, **1b**–**5b** and **1c**–**5c**) were tested with the same concentrations in DMSO solution (0.1 µg/µL). Ligands, complexes and antibiotics indicated varying degrees of inhibitory effects on the growth of different tested both gram negative and gram positive pathogenic bacteria and yeast (Figs. 6, 7).

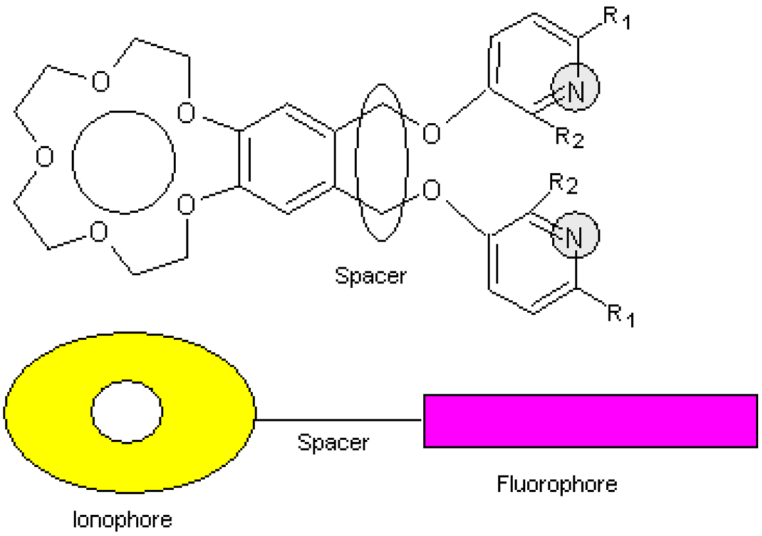

Scheme 5 Representation of PET compounds

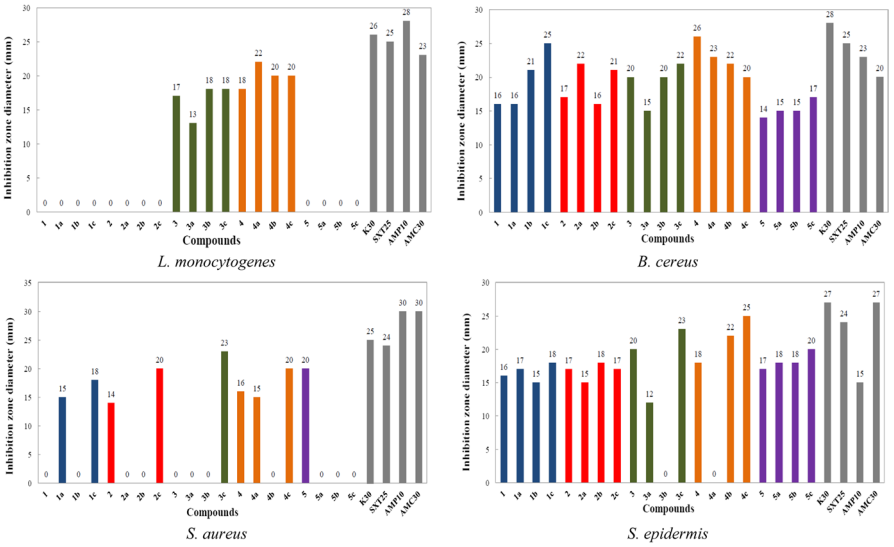

Fig. 6 Antimicrobial activity of ligands (**1–5**) and complexes (**1a–5a**, **1b–5b** and **1c–5c**) and standard reagents (diameter of zone inhibition (mm). SXT25, sulphamethoxazole 25 µg; AMP10, ampicillin 10 µg; K30, kanamycin 30 µg; AMC30, amoxycillin 30 µg

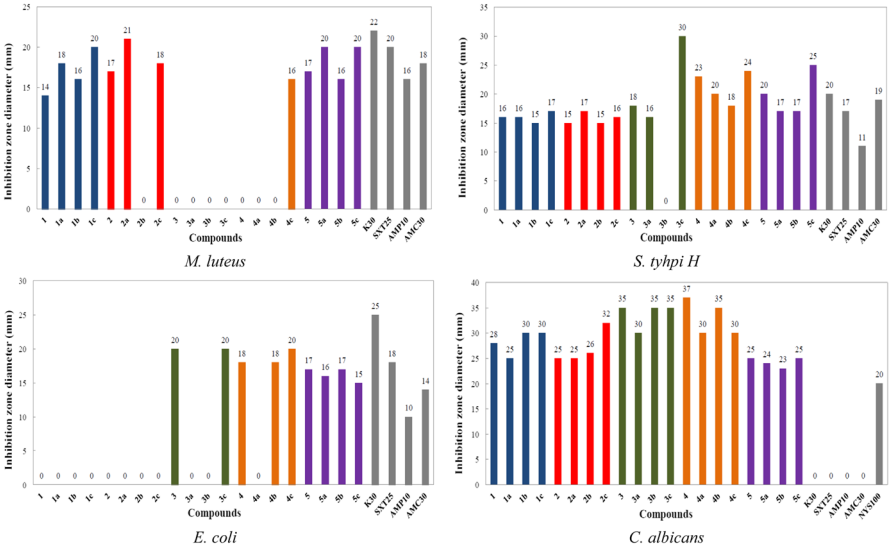

Fig. 7 Antimicrobial activity of ligands (**1–5**) and complexes (**1a–5a**, **1b–5b** and **1c–5c**) and standard reagents (diameter of zone inhibition (mm). SXT25, sulphamethoxazole 25 µg; AMP10, ampicillin 10 µg; NYS100, nystatin 100 µg; K30, kanamycin 30 µg; AMC30, amoxycillin 30 µg

Based on Figs. 6 and 7 results, functional substitutions on the pyridine ring selectively increase or decrease inhibition of ligand's activity. The substituents (CH_3, NO_2, Cl and Br) on the pyridine group seem to be a highly significant factor in influencing the biological activity of the compound. For example, compound **2a** showed the most activity against *M. luteus* (21 mm). However, halogen-substituted (Cl and Br) compounds (**3** and **4**) and their complexes (**3a**, **3b**, **3c**, **4a** and **4b** except **4c**) have been no effect against *M. luteus*. In addition, *L. monocytogenes*, shows selectivity only for halogen-substituted ligands (**3** and **4**) and complexes (**3a**, **3b**, **3c**, **4a**, **4b**, **4c**). This result demonstrates the importance of the substituent bound to the structure for antimicrobial activity [64]. The compounds (**3** and **4**) that have electron-withdrawing groups Cl and Br were more active than those that have electron donating group (CH_3) in compound (**2**) [65]. However, NO_2 substituted (electron withdrawing group) compound **2** and complexes were interestingly inactive for *L. monocytogenes*. *Listeria monocytogenes*, which is commonly found in nature in the genus Listeria, is a highly pathogenic species for humans and animals.

All synthesized ligands (**1**–**5**) and complexes (**1a**–**5a**, **1b**–**5b** and **1c**–**5c**) showed best antibacterial activity against *B. cereus*. Compound **4** showed the most activity against *B. cereus* (26 mm). All of potassium complexes (**1b**–**5b**) were not effective against *S. aureus*. Compound **4c** showed the most activity against *S. epidermis* (25 mm). *S. epidermis* infections are associated with intravascular devices (prosthetic heart valves, etc.) and generally occur in prosthetic joints, catheters and large wounds. This pathogenic microorganism gains resistance against traditional antibiotics every day. There is a need for more effective antibiotics to treat against this disease [36].

Salmonella serovars cause very diverse clinical symptoms, from asymptomatic infection to serious typhoid-like syndromes in infants or certain highly susceptible animals [35, 37]. Compounds **4**, **4c**, **5c** (23 mm, 24 mm, 25 mm, respectively) and especially **3c** were the most potent growth inhibitors against *S. typhi H* with a zone value of 30 mm. Only compound **3b** was not effective for *S. typhi H*. Ligands (**1** and **2**) and their complexes (**1a**, **2a**, **1b**, **2b**, **1c** and **2c**) are completely inactive against *E. coli*. Cl, Br and NO_2 substituted (electron withdrawing groups on pyridine) ligands and complexes (**3**, **3c**, **4**, **4b**, **4c**, **5**, **5a**, **5b** and **5c**) have moderate activity for *E. coli.* It is well known that silver ions and silver-based compounds are highly toxic to microorganisms showing strong biocidal effects on many species of bacteria including *E. coli* [66–68]. However, it is reported that the concentration of the applied compounds and the number of bacteria (CFU) may affect the antimicrobial activity [68]. In our study, this is thought to be the case (Fig. 7). The silver complexes (**1c**–**5c**) have broad antimicrobial activity, which are generally considered the reference standard for the comparison of the growth inhibitory effects of the test materials against Gram-positive bacteria *B. cereus*, *S. epidermis* and Gram-negative bacteria *E. coli* (Figs. 6, 7).

Compound **2a** showed the most activity against *M. luteus* (21 mm). Compound **4c** showed the most activity against *S. epidermis* (25 mm) (Fig. 6). *S. epidermis* which infections are associated with intravascular devices (prosthetic heart valves, etc.), but also generally occur in prosthetic joints, catheters and large wounds. These pathogenic microorganisms gain resistance against traditional

antibiotics every day. There is a need for more effective antibiotics for the treatment of this disease [69]. Compound **4** showed the most activity against *B. cereus* (26 mm).

Systemic fungal infections, including those by *Candida albicans* have emerged as important causes of morbidity and mortality in immune compromised patient (Aids, cancer chemotherapy, organ or bond transplantation) [35]. All the synthesized compounds demonstrated much activity against this yeast. Further, compounds **1b, 1c, 2c, 3**, **3b, 3c, 4, 4a, 4b** and **4c** showed the most inhibition activity against *C. albicans* as compounds with zone values of 30–37 mm. Meanwhile, compound **4** (37 mm) showed the highest activity. In fact, all the synthesized ligands and complexes showed more activity against *C. albicans* than commercial (standard) antifungal (positive control NYS100P) (Fig. 7).

Conclusions

In this study, a series of new double armed ligands (**1–5**) and sodium, potassium and silver(I) complexes (**1a–5a**, **1b–5b** and **1c–5c**) were synthesized and characterized by using analytical and spectral techniques. Pyridine substituted crown ether compounds (**1–5**) were prepared by the reaction of 4′,5′-bis(bromomethyl)benzo-15-crown-5 with hydroxypyridine derivatives in basic media. The chemosensing behavior of **1–5** was carried out using fluorescence spectroscopy. The fluorescence experiments show that the fluorescence emission of **1–5** could be quenched by the addition of Fe^{3+} and Cu^{2+} ion in the ligand. These fluorescence quenching properties of Fe^{3+} and Cu^{2+} ion present a potential for the design of fluorescence sensory materials. The synthesized compounds (**1–5**, **1a–5a**, **1b–5b** and **1c–5c)** have been found to exhibit antibacterial and antifungal activities at moderate to good levels both gram negative and gram positive bacteria. The antimicrobial activity of these compounds was also compared with commercial (standard) antibiotics. It was seen that the synthesized compounds were effective as the antibiotics and antifungal mentioned. Furthermore, some of the synthesized compounds (*S. typhi* H; **3c**, **4**, **4c**, **5c** 30 mm, 23 mm, 24 mm, 25 mm respectively) have been found to be more effective than antibiotics and antifungal (*C. albicans*; all compounds, 23–37 mm). As a result, synthesized molecules may become potential candidates for the clinical trials.

Supporting information available

Tables; experimental details, IR and ^{13}C NMR and also spectra; ^{1}H-NMR, mass and UV–vis spectra of compounds are provided as supplementary material.

Acknowledgements The authors gratefully acknowledge the financial assistance of the Scientific and Technical Research Council of Turkey (TUBITAK), Grant No. TBAG 210T122, and Ankara University Grant No. 17B0430004.

References

1. C.J. Pedersen, J. Am. Chem. Soc. **89**, 7017 (1967)
2. N.S. Poonia, A.V. Bajaj, Chem. Rev. **79**, 389 (1979)
3. F. Vögtle, E. Weber, in *Crown Ethers and Analogs*, ed. by S. Patai, Z. Rappoport (Wiley, Chichester, 1989), p. 207
4. Z. Hayvali, N. Gündüz, Z. Kiliç, E. Weber, J. Prakt. Chem. **341**, 568 (1999)
5. C. Sousa, C. Freire, B. De Castro, Molecules **8**, 894 (2003)
6. D. Liu, K. Tang, W. Liu, C. Su, X. Yan, M. Tan, Y. Tang, Dalton Trans. **39**, 9763 (2010)
7. K. Sako, T. Kakehi, S. Nakano, H. Oku, X.F. Shen, T. Iwanaga, M. Yoshikawa, K. Sugahara, S. Toyota, H. Takemura, T. Shinmyozu, M. Shiotsuka, H. Tatemitsu, Tetrahedron Lett. **55**, 749 (2014)
8. B. Valeur, I. Leray, Coord. Chem. Rev. **205**, 3 (2000)
9. Q.Z. Yang, L.Z. Wu, H. Zhang, B. Chen, Z.X. Wu, L.P. Zhang, C.H. Tung, Inorg. Chem. **43**, 5195 (2004)
10. E.N. Ushakov, M.V. Alfimov, S.P. Gromov, Macroheterocycles **3**, 189 (2010)
11. H.S. Seo, S.H. Lee, J. Fluoresc. **21**, 747 (2011)
12. L. Zhao, X. Chen, F. Guo, B. Gou, C. Yang, W. Xia, J. Lumin. **145**, 486 (2014)
13. J.-P. Malval, R. Lapouyade, Helv. Chim. Acta **84**, 2439 (2001)
14. S.K. Kim, M.Y. Bang, S.-H. Lee, K. Nakamura, S.-W. Cho, J. Yoon, J. Incl. Phenom. Macrocycl. Chem. **43**, 71 (2002)
15. D. Şahin, H. Yılmaz, Z. Hayvalı, Res. Chem. Intermed. **42**, 6337 (2016)
16. D. Şahin, Y. Süzen, Z. Hayvalı, Hetoroatom Chem. **25**, 43 (2014)
17. H. Güler, Z. Hayvali, H. Dal, T. Hökelek, Polyhedron **31**, 688 (2012)
18. K.K. Haldar, T. Sen, A. Patra, J. Phys. Chem. C **114**, 4869 (2010)
19. Z. Hayvalı, H. Güler, H. Öğütcü, N. Sarı, Med. Chem. Res. **23**, 3652 (2014)
20. G.W. Gokel, W.M. Leevy, E. Weber, Chem. Rev. **104**, 2723 (2004)
21. M. Kralj, L. Tusek-Bozic, L. Frkanec, Chem. Med. Chem. **3**, 1478 (2008)
22. P.L. Caradoc-Davies, L.R. Hanton, W. Henderson, J. Chem. Soc. Dalton Trans. **19**, 2749 (2001)
23. Y. Kang, S.S. Lee, K.-M. Park, S.H. Lee, S.O. Kang, J. Ko, Inorg. Chem. **40**, 7027 (2001)
24. C. Seward, J. Chan, D. Song, S. Wang, Inorg. Chem. **42**, 1112 (2003)
25. W. Sun, Y. Cui, H. Liu, H. Zhao, W. Zhang, J. Mol. Struct. **1026**, 133 (2012)
26. T. Nakamura, K. Takeuchi, JP Patent 2003-238832A, 2003
27. N. Kinarivala, P.C. Trippier, Tetrahedron Lett. **55**, 5386 (2014)
28. T.F. Spande, H.M. Garraffo, M.W. Edwards, H.J.C. Yeh, L. Pannell, J.W. Daly, J. Am. Chem. Soc. **114**, 3475 (1992)
29. J.K. Lynch, M.W. Holladay, K.B. Ryther, H. Bai, C.N. Hsiao, H.E. Morton, D.A. Dickman, W. Arnold, S.A. King, Tetrahedron-Asymmetr. **9**, 2791 (1998)
30. J. Li, D. Yim, W.-D. Jang, J. Yoon, Chem. Soc. Rev. **46**, 2437 (2017)
31. V.K. Gupta, S. Chandra, S. Agarwal, Indian J. Chem. **42**, 813 (2003)
32. M.J. Calverley, J. Dale, Acta Chem. Scand. B. **36**, 241 (1982)
33. B. Winkler, A.W.-H. Mau, L. Dai, Phys. Chem. Chem. Phys. **2**, 291 (2000)
34. A. Bilgin, B. Ertem, P. Dinc Agın, Y. Gok, S. Karslıoglu, Polyhedron **25**, 3165 (2006)
35. H. Öğütcü, N.K. Yetim, E.H. Özkan, O. Eren, G. Kaya, N. Sarı, A. Dişli, Pol. J. Chem. Technol. **19**, 74 (2017)
36. C. Nithya, B. Gnanalakshmi, S.K. Pandian, Mar. Environ. Res. **71**, 283 (2011)
37. U. Schillinger, F.K. Lucke, Appl. Environ. Microbiol. **55**(8), 1901 (1989)
38. M. Balouiri, M. Sadiki, K.S. Ibnsouda, J. Pharm. Anal. **6**, 79 (2016)
39. S. Magaldi, S. Mata-Essayag, C. Hartung de Capriles, C. Perez, M.T. Colella, C. Olaizola, Y. Ontiveros, Int. J. Infect. Dis. **8**, 39 (2004)
40. C. Valgas, S.M. De Souza, E.F.A. Smânia, A. Smânia Jr., Braz. J. Microbiol. **38**, 369 (2007)
41. Y. Xiang, X. Liu, C. Mao, X. Liu, Z. Cui, X. Yang, K.W.K. Yeung, Y. Zheng, S. Wu, Mater. Sci. Eng. C **85**, 214 (2018)
42. Z. Liu, Y. Zhu, X. Liu, K.W.K. Yeung, S. Wu, Colloids Surf. B **151**, 165 (2017)
43. Y. Zhu, X. Liu, K.W.K. Yeung, P.K. Chu, S. Wu, Appl. Surf. Sci. **400**, 14 (2017)
44. C. Mao, Y. Xiang, X. Liu, Z. Cui, X. Yang, K.W.K. Yeung, H. Pan, X. Wang, P.K. Chu, S. Wu, ACS Nano **11**, 9010 (2017)
45. E. Bozkır, N. Sarı, H. Ögütcü, J. Inorg. Organomet. Polym. Mater. **22**, 1146 (2012)

46. N. Sarı, N. Pişkin, H. Öğütcü, N. Kurnaz, Med. Chem. Res. **22**, 580 (2013)
47. D. Nartop, N. Sarı, H. Öğütcü, Chin. J. Inorg. Chem. **30**, 921 (2014)
48. A. Altundas, N. Sarı, N. Colak, H. Ögütcü, Med. Chem. Res. **19**, 576 (2010)
49. D. Nartop, N. Sarı, A. Altundas, H. Ögütcü, J. Appl. Polym. Sci. **125**, 1796 (2012)
50. M. Barboiu, A. Mefrfre, Y.-M. Legrand, E. Petit, L. Marin, M. Pinteala, A.V.D. Lee, Supramol. Chem. **26**, 223 (2014)
51. N.S. Poonia, P. Bagdi, K.S. Sidhu, J. Incl. Phenom. **4**, 43 (1986)
52. B. Antonioli, D.J. Bray, J.K. Clegg, K. Gloe, K. Gloe, O. Kataeva, L.F. Lindoy, J.C. McMurtrie, P.J. Steel, C.J. Sumby, M. Wenzel, Dalton Trans. **40**, 4783 (2006)
53. G. Socrates, *Infrared and Raman Characteristic Group Frequencies: Tables and Charts*, 3rd edn. (Wiley, Chichester, 2001)
54. D. Lin-Vien, N.B. Colthup, W.G. Fateley, J.G. Graselli, *The Handbook of Infrared and Raman Characteristic Frequencies of Organic Molecules* (Academic Press, San Diego, 1991)
55. N. Ghildiyal, G.J. Nee Pant, M.S.M. Rawat, K. Singh, Spectrochim. Acta A **171**, 507 (2017)
56. Y. Liu, J.R. Han, H.Y. Zhang, Supramol. Chem. **16**, 247 (2004)
57. Z. Hayvalı, P. Köksal, J. Incl. Phenom. Macrocycl. Chem. **76**, 369 (2013)
58. C.J. Pedersen, H.K. Frensdorff, Angew. Chem. Internat. Edit. **11**, 16 (1972)
59. P.R. Mallison, M.R. Truter, J. Chem. Soc. Perkin **2**, 1818 (1972)
60. V.W. Bhagwat, H. Manohar, N.S. Poonia, Inorg. Nucl. Chem. Lett. **17**, 207 (1981)
61. R. Ziessel, L. Bonardi, P. Retailleau, G. Ulrich, J. Org. Chem. **71**, 3093 (2006)
62. S. Imama-Reja, N. Kumar, R. Sachdeva, V. Bhalla, M. Kumar, RSC Adv. **3**, 17770 (2013)
63. V. Bojinov, N. Georgiev, J. Chem. Technol. Metall. **46**, 3 (2011)
64. F.R.F. Dias, J.S. Novais, T.A. do Nascimento Santos Devillart, W.A. da Silva, M.O. Ferreira, R.S. Loureiro, V.R. Campos, V.F. Ferreira, M.C.B.V. de Souza, H.C. Castro, A.C. Cunha, Eur. J. Med. Chem. **156**, 1 (2018)
65. N.B. Reddy, G.V. Zyryanov, G.M. Reddy, A. Balakrishna, A. Padmaja, V. Padmavathi, C.S. Reddy, J.R. Garcia, G. Sravya, J. Heterocycl. Chem. https://doi.org/10.1002/jhet.3435
66. Z. Xu, X. Wang, X. Liu, Z. Cui, X. Yang, K.W.K. Yeung, J.C. Chung, P.K. Chu, S. Wu, ACS Appl. Mater. Interfaces **9**, 39657 (2017)
67. X. Xie, C. Mao, X. Liu, Y. Zhang, Z. Cui, X. Yang, K.W.K. Yeung, H. Pan, P.K. Chu, S. Wu, ACS Appl. Mater. Interfaces **9**, 26417 (2017)
68. I. Sondi, B. Salopek-Sondi, J. Colloid Interface Sci. **275**, 177 (2004)
69. A. Altundas, Y. Erdogan, H. Ögütcü, H.E. Kizil, G. Agar, Fresenius Environ. Bull. **25**, 5411 (2016)